

Lepton sourced baryon asymmetry in the fourth generation model

Hsiang-nan Li*

Institute of Physics, Academia Sinica, Taipei, Taiwan 115, Republic of China

(Dated: January 30, 2026)

We demonstrate that the observed baryon asymmetry in the Universe can be accommodated in the extended Standard Model with sequential fourth generation fermions (SM4). We first construct the dimension-6 effective operators of the type $-i(\Phi^\dagger\Phi)\bar{F}_L\Phi f_R$ induced by fourth generation quarks, which carry the CP violation (CPV) source from the 4×4 Cabibbo-Kobayashi-Maskawa (CKM) matrix, Φ (F_L , f_R) being a Higgs double (left-handed fermion doublet, right-handed fermion singlet). The required inputs of the fourth generation fermion masses were derived in our previous dispersive analyses on heavy quark decays and neutral meson mixing. The similar framework allows the determination of the 4×4 CKM matrix elements $V_{ib'}$, $i = u, c$ and t , such that the strength of the CPV source can be evaluated unambiguously. The dimension-6 operators associated with fourth generation leptons, as implemented into the formalism for the electroweak baryogenesis in the literature, lead to the baryon-over-entropy ratio $\eta_B \approx 10^{-10}$.

I. INTRODUCTION

The dispersive analyses on the flavor structure of the Standard Model (SM) [1–4] have suggested that the mass hierarchy and the distinct mixing patterns of quarks and leptons are governed by the analyticity of SM dynamics. Our series of works echoes the “S-matrix bootstrap conjecture” advocated by Geoffrey Chew in 1960s [5] that a well-defined but infinite set of self-consistency conditions (based on analyticity, unitarity, causality, etc.) determines uniquely the aspects of particles in nature [6, 7]. The bootstrap conjecture was proposed for strong interaction originally, and then extended to electroweak interaction [8]. Motivated by the dynamical interpretation of the SM flavor structure, we explored the sequential fourth generation model as the most economical extension of the SM (SM4), to which no free parameters are added [9, 10]. For example, the mass $m_{t'} \approx 200$ TeV ($m_{b'} = 2.7$ TeV) of a fourth generation quark t' (b') was demanded by the dispersion relations for the mixing between the neutral quark states $t'\bar{u}$ and $\bar{t}'u$ ($b'\bar{d}$ and $\bar{b}'d$) [9]. The multiple intermediate channels involved in the responsible box diagrams, i.e., the db' , sb' and bb' (ut and ct) channels in the t' (b') case, give consistent results. The mass $m_{\tau'} = 270$ GeV ($m_4 = 170$ GeV) of a fourth generation charged (neutral) lepton τ' (ν') was predicted by investigating the dispersion relation for the decay $\tau' \rightarrow \nu\bar{t}d$ ($t \rightarrow de^+\nu'$), ν (e^+) being a light neutrino (a positron) [10].

We have demonstrated that the heavy quark condensate $\langle \bar{t}'t' + \bar{b}'b' \rangle < 0$ is established as the Yukawa coupling exceeds the critical value $g_Q^c \approx 9.1$ [11]. The heavy quark condensate, producing a quadratic term $\mu^2\phi^2/2$ with the mass parameter $\mu^2 < 0$ in the Higgs potential, breaks the electroweak symmetry [13, 14]. Fourth generation leptons with the smaller Yukawa couplings of $O(1)$ do not constitute the condensate. Additional heavy scalars (or pseudoscalars) then appear as bound states [12] of t' and b' quarks with the masses above a TeV scale in a Yukawa potential (the Yukawa coupling 9.1 corresponds to a quark mass 1.6 TeV). The contributions from $\bar{b}'b'$ scalars to the Higgs boson production via gluon fusion and to the Higgs decay into a photon pair were found to be of $O(10^{-3})$ and $O(10^{-2})$ of the top quark one [9], respectively. Other heavier scalars contribute even less. These estimates elucidated why superheavy fourth generation quarks bypass the experimental constraints from Higgs boson production and decay [15]. Fourth generation leptons, with the masses of the electroweak scale, are too light to form bound states. We evaluated the contribution from charged leptons to the $H \rightarrow \gamma\gamma$ decay width $\Gamma_{\gamma\gamma}$, and evinced that its effect is within the current uncertainties of $\Gamma_{\gamma\gamma}$ measurements. The impact on the oblique parameters from fourth generation quarks and leptons, based on the formulas in [16], is also permitted by the experimental errors. The search for heavy leptons at colliders with the mass of the electroweak scale was simulated in [17, 18].

It has been known that the baryon asymmetry in the Universe (BAU) requires three necessary conditions [19]: baryon number violation, C and CP violation, and departure from thermal equilibrium. Whether the BAU can be understood in the SM was examined in the literature [20–24]. The SM provides the baryon number violating sphaleron interaction, the CP violation (CPV) source from the Kobayashi-Maskawa mechanism, and the electroweak phase transition (EWPT), which is, however, not strongly first-order [25–28]. The extra heavy scalars in the SM4 modify the Higgs potential through the one-loop Coleman-Weinberg correction $V_1(\phi)$ at zero temperature [29] and the one-loop temperature-dependent correction $V_T(\phi)$ [30], such that a barrier between the trivial vacuum and a nontrivial

* Corresponding author, E-mail: hnli@phys.sinica.edu.tw

vacuum of the effective Higgs potential is built up. The resultant ratio $\phi_c/T_c \approx 0.9$ [11], where ϕ_c denotes the location of the nontrivial vacuum at the critical temperature T_c , roughly meets the criterion for the strongly first-order EWPT $\phi_c/T_c \gtrsim 1$. That is, fourth generation quarks play a crucial role for achieving the first-order EWPT.

This work will present a quantitative verification that the aforementioned SM4 accounts for the observed BAU. The standard workflow for calculating the BAU within the electroweak baryogenesis (EWBG), from the derivation of semi-classical CPV sources in plasma particle collisions with expanding bubbles, to the formulation of transport equations for particle number densities, and then to the implementation of weak sphaleron effects, is referred to recent reviews [31, 32]. It has been proposed [33, 34] to test EWBG by means of effective CPV operators, instead of engaging cumbersome exercise on individual models explicitly. The dimension-6 effective operators of the type $-i(\Phi^\dagger\Phi)\bar{F}_L\Phi f_R$, Φ (F_L, f_R) being a Higgs double (left-handed fermion doublet, right-handed fermion singlet) were considered in [35]. As noticed in [34], the BAU from the CPV quark operators is inefficient because of the washout by strong sphalerons, and the lepton sourced BAU turns out to dominate [36–38]. The coefficient g_τ/Λ_τ^2 was assumed for the τ lepton operator in [34] with the τ lepton Yukawa coupling g_τ and the new physics scale $\Lambda_\tau = 1$ TeV, which satisfies the experimental constraint from the electron electric dipole moment (EDM) [39]. It was shown that the τ -sourced BAU suffices to accommodate the observed η_B . However, a more recent study based on the assumption of Minimal Flavor Violation gave a negative conclusion [40], so whether the τ -sourced scenario is viable remains unsettled [41, 42] in a phenomenological viewpoint.

We will adopt the approach in [34], and predict the BAU in the SM4. The dimension-6 effective operators are constructed from fourth generation quarks unambiguously with all essential inputs being specified. Their coefficients depend on the fourth generation quark masses, which were obtained in our earlier dispersive analyses as stated before, and on the 4×4 Cabibbo-Kobayashi-Maskawa (CKM) matrix elements, which carries new CP -odd phases. The latter will be deduced in a similar framework applied to the neutral quark state mixing. The coefficients are found to be proportional to g_f/Λ^2 with the Yukawa couplings g_f for the fermions f in the effective operators. The new physics scale $\Lambda \approx 16$ TeV, being universal for all flavors f , is much higher than $\Lambda_\tau = 1$ TeV set in [34], implying that the τ -sourced BAU is short by two orders of magnitude in our setup. It will be elaborated that the effective operators for fourth generation leptons τ' and ν' , whose contributions are enhanced by the $O(1)$ Yukawa couplings, replace the τ operator in [34]; the implementation of the τ' and ν' operators into the formalism for the EWBG [34] yields the baryon-over-entropy ratio $\eta_B \approx 10^{-10}$ in agreement with the observation.

The rest of the paper is organized as follows. The relevant dimension-6 effective operators are established in Sec. II by matching them to the diagrams consisting of fourth generation quarks in the full theory. It will be seen that the CPV source from the 4×4 CKM matrix is introduced at the three-loop level, and the associated Jarlskog invariant appears naturally. The 4×4 CKM matrix elements V_{ub}, V_{cb} and V_{tb} are acquired in Sec. III by solving the dispersive constraints from the $c\bar{u}-\bar{c}u$, $t\bar{u}-\bar{t}u$ and $t\bar{c}-\bar{t}c$ neutral quark state mixings. Given the 4×4 CKM matrix elements and the coefficients g_f/Λ^2 of the dimension-6 operators, we extract the prediction for the BAU straightforwardly from the results in [34] in Sec. IV. Section V contains the summary: fourth generation quarks make the first-order EWPT through the interactions between their bound-state scalars and Higgs bosons, and fourth generation leptons create the BAU through their CPV scattering with emergent bubbles during the first-order EWPT. Appendix A collects the details of attaining the dimension-6 effective operators with the CPV source. We take this opportunity to reanalyze the 4×4 Pontecorvo–Maki–Nakagawa–Sakata (PMNS) matrix for the lepton mixing in Appendix B, confirming the outcomes for the involved mixing angles and CP phase in our previous publication [10].

II. EFFECTIVE OPERATORS

It has been recognized that new physics is requested to achieve the first-order EWPT and to enhance CPV, which are the necessary conditions for realizing the BAU. An effective theory, allowing a model-independent and systematic investigations of relevant new physics impacts, has been probed intensively in the literature [43–45]; an effective $\phi^6/(8M^2)$ term, M being a new physics scale, was introduced into the Higgs potential to prompt the first-order EWPT. As to the CPV, the dimension-6 operators in the form $-i(\Phi^\dagger\Phi)\bar{F}_L\Phi f_R$ with an imaginary coefficient were proposed [46], whose strength was constrained by available experimental data for the electron EDM. The new CPV sources were then included into the transport equations that describe interactions between SM plasma particles and bubbles emerging during the first-order EWPT. The particle number densities were solved from the transport equations, and the BAU from the top quark source was calculated [33]. We take advantage of the above formalism, constructing the dimension-6 effective operators with definite coefficients based on our SM4 setup and reading off the predictions for the BAU that correspond to the strength of the effective operators. This strategy saves the tedious handling of transport processes and sphaleron effects [47] specific to the SM4.

The aforementioned effective operators appear in certain renormalizable extensions of the SM, such as models with vector-like quarks and Higgs triplets [48]. We illustrate that fourth generation quarks also produce the $\phi^6/(8M^2)$ term

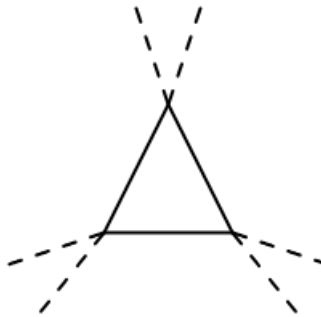


FIG. 1: Diagram for producing the dimension-6 effective operator $\phi^6/(8M^2)$, where a dashed (solid) line represents a Higgs boson (heavy scalar).

with the desired strength. This is expected, since our SM4 setup has been shown to induce the first-order EWPT [11]. Firstly, the Higgs-heavy-quark interaction could be replaced by the effective interaction $\lambda'\phi^2\eta^2/2$ in the symmetry broken phase, where the coupling takes a value $\lambda' \approx 3.8$ [11] and η denotes a bound-state scalar formed by fourth generation quarks. We then derive the dimension-6 operator by integrating out the η field at the electroweak scale. The triangular diagram in Fig. 1 with six external Higgs legs leads to the effective vertex

$$\frac{-i}{8M^2} = 8 \frac{(2\lambda')^3}{3!} \int \frac{d^4 l}{(2\pi)^4} \left(\frac{1}{l^2 - m_\eta^2} \right)^3, \quad (1)$$

where the coefficient 8 is from the combinatorial factor, $2\lambda'$ is associated with the $\phi^2\eta^2$ vertex, and $1/3!$ comes with the expansion to the third power of the interaction term. The momenta of external Higgs bosons, being of order of the electroweak scale and much lower than the heavy scalar mass $m_\eta \approx 3.2$ TeV [9], have been neglected. A simple computation of the integral in Eq. (1) gives

$$M = \sqrt{\frac{3}{8\lambda'^3} \pi m_\eta} \approx 830 \text{ GeV}. \quad (2)$$

Referring to Fig. 1 in [43], we see that the point $(m_H, M) = (125, 830)$ in units of GeV is near the the curve labeled by $\xi \equiv \phi_c/T_c = 1$. This observation coincides with the one in [11] that our SM4 setup generates the first-order EWPT characterized by ξ around unity. The consistency encourages our attempt to translate the SM4 into the effective theory in [43, 44].

The dimension-6 effective operator $-is_f g_f (\Phi^\dagger \Phi) \bar{F}_L \Phi f_R / \Lambda^2$ results in, after the electroweak symmetry breaking,

$$-i \frac{s_f g_f v^2}{\sqrt{2}\Lambda^2} \phi \bar{f} \gamma_5 f, \quad (3)$$

with the Yukawa coupling g_f of a fermion f [34, 49] and the vacuum expectation value (VEV) v of a Higgs field. The discretionary sign $s_f = +1$ or -1 was chosen to accommodate the observed BAU [34], e.g., $s_t = +1$ for a top quark and $s_\tau = -1$ for a τ lepton. The new physics scale Λ was constrained by the data of the electron EDM, which could vary with the flavor f , depending on the sensitivity of the operator to the data. We will construct the operator in Eq. (3) from the SM4 below. It will be highlighted that both the sign s_f and the new physics scale Λ , i.e., the strength of the operator, are fixed unambiguously by matching Eq. (3) to the full theory with fourth generation quarks.

We explicate that the CPV source of the effective operator arises in three-loop diagrams with fourth generation quarks. It is more convenient to assess heavy quark contributions in the R_ξ gauge than in the unitary gauge. If the latter is employed, the effect from a weak boson exchange between heavy quarks will be governed by the $q_\mu q_\nu$ piece in a weak boson propagator with the momentum q . After applying equations of motion, we have the Yukawa couplings associated with fourth generation quarks, which are much larger than the weak coupling. This contribution is identical to that from the exchange of a charged scalar or a neutral pseudoscalar in the R_ξ gauge. Figure 2(a) displays a fourth generation quark loop, say, a t' loop, with one vertex from a Higgs boson H and another from a pseudoscalar ϕ_Z in a Higgs doublet. The virtual ϕ_Z splits into a fermion pair $f\bar{f}$, developing the pseudoscalar current $\bar{f}\gamma_5 f$. This diagram does not endow a CP -odd phase apparently. We must add charged scalars to Fig. 2(a), whose

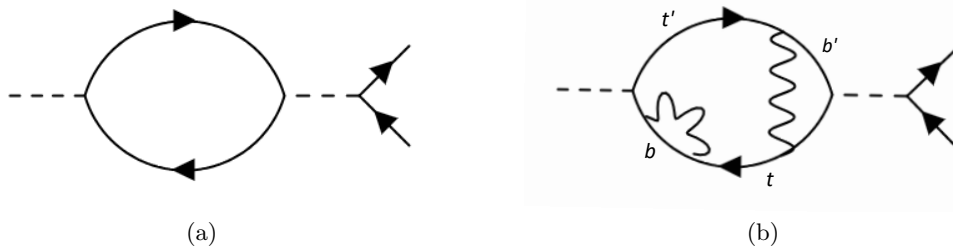


FIG. 2: (a) One-loop diagram and (b) three-loop diagram for the effective operator $\phi \bar{f} \gamma_5 f$, where an arrowed solid line denotes a heavy quark and a wavy line denotes a charged scalar.

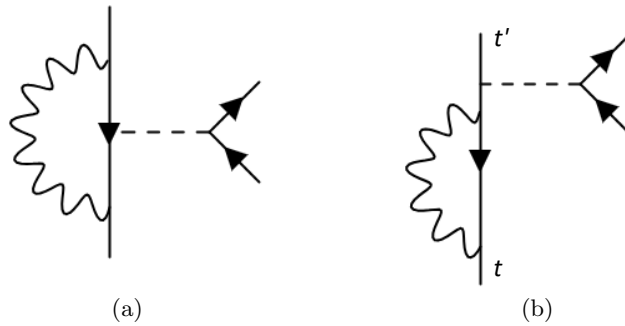


FIG. 3: (a) Vertex correction and (b) self-energy correction contained in the pseudoscalar penguin.

attachments to the t' quark loop bring in 4×4 CKM matrix elements. Adding a single charged scalar does not make an imaginary contribution, for the associated product of the CKM matrix elements, like $V_{t'b'}^* V_{t'b'}$, is real. We need at least two charged scalars.

To maximize the CPV source, the external Higgs boson attaches a t' quark, which has the largest mass $m_{t'}$, i.e., the largest Yukawa coupling $g_{t'}$ among quarks at the electroweak scale. One charged scalar crosses the pseudoscalar vertex, inducing a pseudoscalar penguin for the flavor-changing transition $t' \rightarrow t$ with an internal b' quark. If the internal b' quark is exchanged for a b quark, the CP -odd phase will be down by the lower b quark Yukawa coupling. To form a complete set of penguin diagrams, the self-energy correction from the charged scalar should be included, which also involves the $t' \rightarrow t$ transition with an internal b' quark. In this case, the pseudoscalar attaches the t' , instead of t , quark to keep the contribution maximal. For a similar reason, another charged scalar should form a self-energy correction with the $t \rightarrow t'$ transition, instead of crossing the Higgs boson vertex. Otherwise, the contribution will be suppressed by the b quark Yukawa coupling. The inclusion of the two charged scalars thus gives rise to the three-loop diagram in Fig. 2(b), which contains the sequence of flavor-changing transitions $t' \rightarrow b' \rightarrow t \rightarrow b \rightarrow t'$ with the product of the 4×4 CKM matrix elements $V_{t'b'}^* V_{tb'} V_{tb}^* V_{tb}$. The imaginary part of this product, serving precisely as a Jarlskog invariant [50–52], provides a CPV source. Substituting other lighter up-type (down-type) quarks for t (b) yields minor contributions owing to smaller Yukawa couplings.

We remark that the parametrization in Eq. (3) with the coefficient being proportional to the Yukawa coupling g_f [34] applies to heavy fermions $f = t, \tau', \nu'$, and the CP -odd phase identified above is maximal. For light fermions, the parametrization does not hold in the SM4, because contributions from other types of diagrams may be comparable to that from Fig. 2(b). For instance, changing the virtual pseudoscalar to a virtual Z boson causes a suppression factor $g/g_{b'}$ from the vertex on the internal b' quark line, g being the weak coupling. At the same time, the change brings in an enhancement factor g/g_f from the vertex on the light fermion line of f . The new diagram, generating an electroweak penguin with a $V - A$ current, will not be negligible, if g^2 and $g_{b'} g_f$ are of the similar order of magnitude. The contributions from light fermions to the BAU are expected to be insignificant [34], so we focus only on those from the pseudoscalar currents of the heavy flavors $f = t, \tau', \nu'$, when discussing the BAU in the SM4 below.

Evaluating a three-loop diagram directly is tedious. Our strategy is to build the subdiagrams first, such as the pseudoscalar penguin which involves the vertex correction in Fig. 3(a) and the self-energy correction associated with the $t' \rightarrow t$ transition in Fig. 3(b), and then insert it into the heavy quark loop to get the final result. The two subdiagrams are calculated in Appendix A. We remind that the major source of theoretical uncertainties in the

analysis resides in the formulation the transport equations, so this simplified handling should be acceptable. As illuminated in Appendix A, both Figs. 3(a) and 3(b) exhibit ultraviolet (UV) divergences, which turn out to cancel each other. Furthermore, their contributions cancel exactly in the limit $q^2 \rightarrow 0$, q^2 being the invariant mass of the fermion pair $f\bar{f}$. It indicates that their net contribution is proportional to q^2 , which then removes the pole of the virtual pseudoscalar propagator $1/q^2$ in the R_ξ gauge with the gauge parameter $\xi = 0$, making a four-fermion operator $\bar{t}(1 + \gamma_5)t'(\bar{f}\gamma_5 f)$. Namely, the pseudoscalar penguin diagrams produce a four-fermion operator like the QCD and electroweak penguins in the effective weak Hamiltonian, whose appearances are warranted by the gauge invariance [53].

The pseudoscalar penguin contribution derived in Appendix A reads

$$P = -\frac{i}{192} V_{t'b'}^* V_{tb'} I_{3b'} I_{3f} \frac{g_f g_{b'}^2 g_{t'}}{m_{b'}^2} (1 + \gamma_5) \bar{f}(q_2) \gamma_5 f(q_1), \quad (4)$$

where the external t' and t quark legs have been truncated, and $I_{3b'}$ (I_{3f}) is the third component of the b' quark (f fermion) isospin. Appendix A also presents the expression for the self-energy correction associated with the $t \rightarrow t'$ transition,

$$S = \frac{i}{64\pi^2} V_{tb}^* V_{t'b} g_{t'} g_t \left(\ln \frac{\Lambda_s^2}{-p^2} + 1 \right) \not{p} (1 + \gamma_5), \quad (5)$$

with the t quark momentum p . The electroweak symmetry restoration scale Λ_s is introduced through the upper bound of the loop momentum, below which the full theory with massive fourth generation quarks makes sense.

We then come to the second step, computing the heavy quark loop with the insertions of the pseudoscalar penguin P and the self-energy correction S . The loop integral with the CP -odd phase is written as

$$\begin{aligned} \Pi &= -\frac{i}{64\pi^2} g_{t'} g_t \frac{-i}{192} I_{3b'} I_{3f} \frac{g_f g_{b'}^2 g_{t'}}{m_{b'}^2} \int \frac{d^4 l}{(2\pi)^4} \left(\ln \frac{\Lambda_s^2}{-l^2} + 1 \right) \\ &\quad \times \text{Tr} \left[i \not{l} (1 + \gamma_5) \frac{i(\not{l} + m_t)}{l^2 - m_t^2} (1 + \gamma_5) \frac{i(\not{l} + m_{t'})}{l^2 - m_{t'}^2} \frac{-ig_{t'}}{\sqrt{2}} \frac{i(\not{l} + m_{t'})}{l^2 - m_{t'}^2} \right] J \bar{f} \gamma_5 f, \end{aligned} \quad (6)$$

where the first minus sign on the right-hand side is attributed to the fermion loop, and Tr refers to the traces over the fermion and color flows. The external momentum from the Higgs boson and the electroweak-scale masses have been dropped relative to the heavy quark masses, except the t quark mass m_t in the numerator, which survives the trace. The imaginary part of the product of the 4×4 CKM matrix elements,

$$J = \text{Im}(V_{t'b'}^* V_{tb'} V_{tb}^* V_{t'b}), \quad (7)$$

can be visualized as the area of the parallelogram formed by the vectors $V_{t'b'}^* V_{tb'}$ and $V_{tb}^* V_{t'b}$ in a complex plane. The trace gives a factor $4N_c = 12$, N_c being the number of colors. The integral in Eq. (6) reduces to

$$\Pi = \frac{I_{3b'} I_{3f} g_f g_t^2 m_{t'}^4}{32^2 \pi^4 \sqrt{2} v^4} \left[1 + \text{Li}_2 \left(-\frac{\Lambda_s^2}{m_{t'}^2} \right) \right] J \bar{f} \gamma_5 f, \quad (8)$$

where the loop momentum is cut at the restoration scale Λ_s , and the relations $m_{t,b',t'} = g_{t,b',t'} v / \sqrt{2}$ have been employed.

It has been known that the Yukawa couplings of fourth generation quarks evolve with the energy scale; they decrease with the scale as depicted in [11, 13]. The t' quark mass $m_{t'}$ represents a characteristic scale of the heavy quark loop; for example, it characterizes the scale of the $t' \rightarrow t$ pseudoscalar penguin in Fig. 3(a). If $m_{t'}$ was above Λ_s , internal particles in the penguin diagram become massless, so the full theory with massive quarks does not apply. If $m_{t'}$ was much lower than Λ_s , such that b' quarks form deep bound states, the formulation of the full theory is not appropriate either; fourth generation quarks are heavy enough for forming bound states at the electroweak scale as observed in [9]. The above argument suggests to perform the matching between the effective and full theories at the scale, where $m_{t'}$ takes a value right below Λ_s . Hence, we set $m_{t'} = \Lambda_s$, and have $\text{Li}_2(-1) = -\pi^2/12$. Equating the coefficient of the effective operator to Eq. (8) with $I_{3b'} = -1/2$, and defining the constant $c = 1 - \pi^2/12$, we arrive at

$$\frac{s_f g_f v^2}{\sqrt{2} \Lambda^2} = -\frac{c}{2} \frac{I_{3f} g_f g_t^2 \Lambda_s^4 J}{32^2 \pi^4 \sqrt{2} v^4}. \quad (9)$$

The value of the Jarlskog invariant J will be estimated in the next section.

III. 4×4 CKM MATRIX

We have conducted dispersive analyses on the mixing between the neutral quark states $Q\bar{q}$ and $\bar{Q}q$ [3], where Q (q) stands for a massive (light) quark. The case with $Q = c$ and $q = u$ corresponds to the D meson mixing [54, 55]. The only assumption underlying the analyses is that the electroweak symmetry of the SM is restored as the heavy quark mass m_Q is above a high energy scale [56]. It has been demonstrated that this restoration can take place in our SM4 setup [11]. The mixing phenomenon disappears owing to the unitarity of the CKM matrix, as the electroweak symmetry is restored. The disappearance of the mixing at $m_Q > \Lambda_s$, Λ_s being the restoration scale, was then taken as the input to the dispersion relation for the mixing amplitude, whose behavior at low $m_Q < \Lambda_s$, i.e., in the symmetry broken phase, could be solved. It was found that the solution imposes stringent constraints on the quark masses and the CKM matrix elements appearing in the mixing amplitude [3]. The similar formalism applies to the mixing between the lepton states $\mathcal{L}^-\ell^+$ and $\mathcal{L}^+\ell^-$ [3, 4], where \mathcal{L} (ℓ) denotes a massive (light) charged lepton. The case with $\mathcal{L} = \mu$ and $\ell = e$ corresponds to the mixing of muonia μ^-e^+ and μ^+e^- . Some of our observations are that the normal ordering of the neutrino masses is favored, and that the smaller mixing angles in the quark sector than in the lepton sector are due to the hierarchical mass ratios $m_s^2/m_b^2 \ll m_2^2/m_3^2$, where m_s , m_b , m_2 and m_3 are the masses of a strange quark, a bottom quark, a second-generation neutrino and a third-generation neutrino, respectively.

We extend the dispersive study on the 3×3 CKM matrix in [3] to the one on the 4×4 matrix. The lower mixing angles in the quark sector justify the Wolfenstein parametrization, i.e., the expansion of the CKM matrix elements in the Wolfenstein parameter λ . We follow the parametrization of the 4×4 CKM matrix elements associated with fourth generation quarks in [57],

$$V_{ub'} = p\lambda^3 e^{-i\delta'}, \quad V_{cb'} = q\lambda^2 e^{-i\delta''}, \quad V_{tb'} = r\lambda, \quad (10)$$

up to leading powers of λ . A 3×3 (4×4) unitary matrix depends on three angles and one CP -odd phase (six angles and three CP -odd phases). We will treat the four parameters in the 3×3 CKM matrix as inputs and solve for the remaining five unknowns p , q , r , δ' and δ'' . We have ensured that the alternative parametrization with δ'' assigned to $V_{tb'}$ leads to the same Jalskog invariant.

We prepare the other matrix elements in powers of λ to the desired accuracy, quoting the results in [58],

$$V_{ud} = 1 - \frac{\lambda^2}{2} - \frac{\lambda^4}{8}, \quad V_{us} = \lambda, \quad V_{ub} = A\lambda^3 C e^{-i\delta}, \quad (11)$$

with

$$C = \sqrt{\rho^2 + \eta^2} \approx \frac{\sqrt{\rho^2 + \bar{\eta}^2}}{1 - \lambda^2/2} \quad (12)$$

in terms of the conventional parameters ρ and η , and the weak phase δ in the 3×3 CKM matrix. Equation (11) together with $V_{ub'}$ in Eq. (10) obey the unitarity condition for the first row of the matrix up to corrections of $O(\lambda^6)$. The impact on V_{ud} from the additional $V_{ub'}$ starts at $O(\lambda^6)$,

$$V_{ud} = 1 - \frac{\lambda^2}{2} - \frac{\lambda^4}{8} - \frac{\lambda^6}{16}(1 + 8A^2C^2 + 8p^2), \quad (13)$$

which improves the unitarity condition up to corrections of $O(\lambda^7)$.

The elements of the second row are written as

$$\begin{aligned} V_{cd} &= -\lambda + \frac{\lambda^5}{2}(A^2 + q^2 - 2A^2Ce^{i\delta} - 2pqe^{i\delta' - i\delta''}), \\ V_{cs} &= 1 - \frac{\lambda^2}{2} - \frac{\lambda^4}{8}(1 + 4A^2 + 4q^2), \quad V_{cb} = A\lambda^2. \end{aligned} \quad (14)$$

It is trivial to verify the unitarity conditions, i.e., the normalization of the second row and its orthogonality to the first row, up to $O(\lambda^5)$. The elements of the third row are given by

$$\begin{aligned} V_{td} &= A\lambda^3(1 - Ce^{i\delta}) + r(qe^{i\delta''} - pe^{i\delta'})\lambda^4 + \frac{A}{2}[(1 + r^2)Ce^{i\delta} - r^2]\lambda^5, \\ V_{ts} &= -A\lambda^2 - qre^{i\delta''}\lambda^3 + \frac{A}{2}(1 + r^2 - 2Ce^{i\delta})\lambda^4 + \frac{1}{2}r(qe^{i\delta''} - 2pe^{i\delta'})\lambda^5, \\ V_{tb} &= 1 - \frac{r^2}{2}\lambda^2 - \frac{1}{8}(4A^2 + r^4)\lambda^4 - Aqr\cos\delta''\lambda^5. \end{aligned} \quad (15)$$

The explicit expressions for the fourth row elements $V_{t'i}$, $i = d, s, b, b'$, can be acquired via the unitarity conditions.

The formulas for the lepton state mixing, such as the $\mu^-e^+ - \mu^+e^-$ muonium mixing, in the SM4 [4] are gathered in Appendix B, where they are reinvestigated incidentally. The dispersive constraints from the quark state mixing on the quark masses and mixing angles are similar, as long as the electroweak symmetry is restored above the scale Λ_s ; one simply replaces the neutrino masses m_1, m_2, m_3 and m_4 in Eqs. (B9)-(B11) and Eq. (B13) by the down-type quark masses m_d, m_s, m_b and $m_{b'}$, respectively. It is obvious that the dispersive constraints can be satisfied by diminishing the common factors in the above equations,

$$\lambda_d \frac{m_{b'}^2 - m_d^2}{m_W^2 - m_d^2} + \lambda_s \frac{m_{b'}^2 - m_s^2}{m_W^2 - m_s^2} + \lambda_b \frac{m_{b'}^2 - m_b^2}{m_W^2 - m_b^2} \approx 0, \quad (16)$$

$$\frac{\lambda_d}{m_W^2 - m_d^2} + \frac{\lambda_s}{m_W^2 - m_s^2} + \frac{\lambda_b}{m_W^2 - m_b^2} \approx 0, \quad (17)$$

with the product of the CKM matrix elements $\lambda_i = V_{Qi}^* V_{qi}$, $i = d, s, b$, and the W boson mass m_W .

We implement the approximation

$$\frac{m_{b'}^2 - m_i^2}{m_W^2 - m_i^2} \approx \frac{m_{b'}^2}{m_W^2} \left(1 - \frac{m_i^2}{m_{b'}^2} + \frac{m_i^2}{m_W^2} \right) \approx \frac{m_{b'}^2}{m_W^2} \left(1 + \frac{m_i^2}{m_W^2} \right) \approx \frac{m_{b'}^2}{m_W^2 - m_i^2}, \quad (18)$$

based on the mass hierarchy $m_i^2 \ll m_W^2 \ll m_{b'}^2$. Equations (16) and (17) then turn into the same relation

$$\lambda_{b'} = \lambda_d \frac{m_d^2}{m_W^2} + \lambda_s \frac{m_s^2}{m_W^2} + \lambda_b \frac{m_b^2}{m_W^2} \approx \lambda_s \frac{m_s^2}{m_W^2} + \lambda_b \frac{m_b^2}{m_W^2}, \quad (19)$$

where the unitarity condition $\lambda_d + \lambda_s + \lambda_b = -\lambda_{b'}$ has been inserted, and the d quark mass m_d has been ignored. Note that Eqs. (16) and (17) stand for two distinct constraints on the lepton mixing, since the masses of a fourth generation neutrino and a W boson are of the same order, and the m_i^2/m_4^2 pieces, $i = 1, 2, 3$, are comparable with m_i^2/m_W^2 . Besides, the masses of down-type quarks (neutrinos) in the intermediate channels of the considered neutral fermion state mixings possess different spectra. The above explain why the dispersion relations produce variant solutions for the CKM and PMNS matrices.

Equation (19) will be utilized to determine the 4×4 CKM matrix elements. The light quark in the proposed heavy-light system is regarded as being massless [3]. We do not include the $t'\bar{u}-\bar{t}'u$ mixing; the mass $m_{t'} \approx 200$ TeV of a superheavy t' quark at the electroweak scale, much higher than the symmetry restoration scale Λ_s definitely [11], renders all internal particles in the box diagrams massless, so the mixing phenomenon disappears. In other words, the $t'\bar{u}-\bar{t}'u$ mixing is not a suitable process for the study. The real and imaginary parts of the dispersion relations in Eq. (19) from the $c\bar{u}-\bar{c}u$ and $t\bar{u}-\bar{t}u$ mixings impose four constraints. To have enough equations for the five unknowns p, q, r, δ' and δ'' , we must take into account the $t\bar{c}-\bar{t}c$ mixing. A tc pair is not a heavy-light system, strictly speaking, to which the present formulas may not hold well. In principle, we should construct a more complicated mixing amplitude for the tc case, in which both external quarks have finite masses. We will not attempt such a rigorous approach here, but treat a charm quark as being massless. The theoretical uncertainty stemming from this approximation is anticipated to be minor relative to those in the formulation for the EWBG.

The $c\bar{u}-\bar{c}u$, $t\bar{u}-\bar{t}u$ and $t\bar{c}-\bar{t}c$ mixing amplitudes, each of which involves real and imaginary parts, offer six relations. That is, our setup is overconstrained. We first exemplify that when the strange quark mass m_s , which can be regarded as the sixth unknown, vanishes, a unique set of solutions for p, q, r, δ' and δ'' can be established. These solutions give an idea on the order of magnitude of the matrix elements associated with a fourth generation. Employing Eqs. (10), (11), (14) and (15), we attain, from Eq. (19),

$$\begin{aligned} p q e^{-i(\delta' - \delta'')} &= \frac{m_b^2}{m_W^2} A^2 C e^{-i\delta}, \\ p r e^{-i\delta'} &= \frac{m_b^2}{m_W^2} \frac{AC}{\lambda} \left(1 - \frac{r^2 \lambda^2}{2} \right) e^{-i\delta}, \\ q r e^{i\delta''} &= \frac{m_b^2}{m_W^2} \frac{A}{\lambda} \left(1 - \frac{r^2 \lambda^2}{2} \right), \end{aligned} \quad (20)$$

for the $c\bar{u}-\bar{c}u$, $t\bar{u}-\bar{t}u$ and $t\bar{c}-\bar{t}c$ mixings, respectively.

It is straightforward to solve for

$$p = \frac{m_b A C}{m_W}, \quad q = \frac{m_b A}{m_W}, \quad r = \frac{m_b}{\lambda m_W}, \quad \delta' = \delta, \quad \delta'' = 0. \quad (21)$$

The values of p , q and r are all of order of m_b/m_W with the inequality $p < q < r$. The second terms $r^2\lambda^2/2$ in the parentheses of Eq. (20), being suppressed by the power m_b^2/m_W^2 compared to the first terms, are negligible. We have the four inputs [59]

$$\lambda \approx 0.225, \quad A \approx 0.826, \quad C \approx 0.397, \quad \delta \approx 1.15, \quad (22)$$

among which the value of λ is precise, A and δ have about 2% uncertainties, and C can vary by 3%. The W boson mass is set to $m_W \approx 80.4$ GeV [59], which has much higher precision. Because our analysis is based on the tree-level expression for the box diagrams, it is more appropriate to choose a scale-independent quark mass. Therefore, we adopt the pole mass $m_b \approx 4.78$ GeV for a b quark with roughly 1% uncertainty [59], deriving the matrix elements in Eq. (10)

$$V_{ub'} \approx 2.22 \times 10^{-4} e^{-1.15i}, \quad V_{cb'} \approx 2.49 \times 10^{-3}, \quad V_{tb'} \approx 5.95 \times 10^{-2}. \quad (23)$$

The results indicate that a more off-diagonal matrix element has a smaller magnitude in consistency with the pattern of the 3×3 matrix.

Next we implement the finite mass m_s , for which one of the six constraints needs to be relaxed. Viewing the smallness of the phase δ'' and the potential uncertainty from ignoring the charm quark mass, we exclude the imaginary part of the constraint from the $t\bar{c}-\bar{t}c$ mixing. Equation (20) becomes

$$\begin{aligned} p q e^{-i(\delta' - \delta'')} &= \frac{m_b^2}{m_W^2} A^2 C e^{-i\delta} + \frac{m_s^2}{m_W^2} \frac{1}{\lambda^4} \\ p r e^{-i\delta'} &= \frac{m_b^2}{m_W^2} \frac{AC}{\lambda} e^{-i\delta} - \frac{m_s^2}{m_W^2} \frac{A}{\lambda}, \\ q r \cos \delta'' &= \frac{m_b^2}{m_W^2} \frac{A}{\lambda} - \frac{m_s^2}{m_W^2} \frac{A}{\lambda}, \end{aligned} \quad (24)$$

where the $r^2\lambda^2/2$ terms have been dropped, and only the m_s -dependent terms leading in powers of λ are retained. It is seen that the m_s -dependent correction mainly occurs in the first relation, which is associated with the large product of the matrix elements $V_{us}^* V_{cs}$. The m_s -dependent terms in the second and third lines have tiny effects.

It is tricky to choose a scale-independent strange quark mass. A pole mass is not well defined for a light quark owing to the unreliable perturbative renormalization-group (RG) evolution at a low scale. We assume that the running coupling constant is frozen at a low scale by, for instance, a gluon mass induced by confinement. In this way the strange quark $\overline{\text{MS}}$ running mass is also frozen, and serves as a scale-independent mass. It is thus reasonable to set the strange quark mass to its $\overline{\text{MS}}$ value at the renormalization scale $\mu = 1$ GeV [59], $m_s = 0.11 \pm 0.02$ GeV with 20% uncertainty, which covers the variation within the range $0.5 \text{ GeV}^2 < \mu^2 < 4.0 \text{ GeV}^2$. The coupled equations are then solved numerically to yield

$$p = 0.0223^{+0.0001}_{-0.0004}, \quad q = 0.0639^{+0.0053}_{-0.0085}, \quad r = 0.231^{+0.015}_{-0.020}, \quad \delta' = 1.15 \pm 0.03, \quad \delta'' = 0.489^{+0.137}_{-0.122}, \quad (25)$$

whose uncertainties originate from those of the Wolfenstein parameters and of the b and s quark masses. The s quark mass is responsible for the dominant source of uncertainties.

The fourth column elements are then given by

$$\begin{aligned} V_{ub'} &= 2.54^{+0.02}_{-0.05} \times 10^{-4} \exp[-(1.15 \pm 0.03)i], \quad V_{cb'} = 3.23^{+0.26}_{-0.43} \times 10^{-3} \exp[-(0.489^{+0.137}_{-0.122})i], \\ V_{tb'} &= 5.20^{+0.34}_{-0.45} \times 10^{-2}. \end{aligned} \quad (26)$$

It is noticed that the inclusion of the s quark mass mainly modifies the phase δ'' , and has negligible impacts on the magnitude of the matrix elements. The evaluation of the Jarlskog invariant in Eq. (7) demands the input of the element $V_{t'b}$. For completeness, we collect our predictions for the fourth row of the 4×4 CKM matrix based on the unitarity,

$$\begin{aligned} V_{t'u} &= 3.16^{+1.05}_{-1.32} \times 10^{-4} \exp[(1.15^{+0.03}_{-0.03})i], \quad V_{t's} = -(1.63^{+0.55}_{-0.69}) \times 10^{-3} \exp[(1.15^{+0.03}_{-0.03})i], \\ V_{t'b} &= -(5.20^{+0.34}_{-0.44}) \times 10^{-2} \exp[(1.22^{+0.44}_{-0.62}) \times 10^{-3}i], \quad V_{t'b'} = 0.999^{+0.001}_{-0.000}. \end{aligned} \quad (27)$$

The above solutions suggest the maximal unitarity violation in the third row of the 3×3 CKM matrix, and the potential of searching for the unitarity violation in B meson decays.

We confront our predictions for the fourth column and row of the 4×4 CKM matrix with those extracted from measurements in the kaon and B meson systems [60],

$$\begin{aligned} |V_{ub'}| &= 0.017 \pm 0.014, \quad |V_{cb'}| = (8.4 \pm 6.2) \times 10^{-3}, \quad |V_{tb'}| = 0.07 \pm 0.08, \\ |V_{t'd}| &= 0.01 \pm 0.01, \quad |V_{t's}| = 0.01 \pm 0.01, \quad |V_{t'b}| = 0.07 \pm 0.08, \quad |V_{t'b'}| = 0.998 \pm 0.006. \end{aligned} \quad (28)$$

It is apparent that the experimental bounds are still loose and broad ranges of the matrix elements are allowed. The bounds on the CP -odd phases are even weaker [60],

$$\delta' = 1.21 \pm 1.59, \quad \delta'' = 1.10 \pm 1.64. \quad (29)$$

The results in Eqs. (26) and (27) comply with the current experimental constraints.

The 2.3σ deviation from the unitarity in the first row of the 3×3 CKM matrix

$$|V_{ud}|^2 + |V_{us}|^2 + |V_{ub}|^2 = 0.9984 \pm 0.0007, \quad (30)$$

was reported [59], known as the Cabibbo angle anomaly. The unitarity of the second row, the first column and the second column of the 3×3 CKM matrix have been scrutinized to the precision of $O(10^{-4}) - O(10^{-2})$ [61, 62] as summarized in [59],

$$\begin{aligned} |V_{cd}|^2 + |V_{cs}|^2 + |V_{cb}|^2 &= 1.001 \pm 0.012, \\ |V_{ud}|^2 + |V_{cd}|^2 + |V_{td}|^2 &= 0.9971 \pm 0.0020, \\ |V_{us}|^2 + |V_{cs}|^2 + |V_{ts}|^2 &= 1.003 \pm 0.012. \end{aligned} \quad (31)$$

Equations (26) and (27) hint what experimental precision need to be reached in order to confirm the deviations [63].

IV. BARYON ASYMMETRY

We then predict the Jarlskog invariant for the CPV source in the dimension-6 operators,

$$J = -(3.30_{-0.85}^{+0.89}) \times 10^{-6}, \quad (32)$$

from the 4×4 CKM matrix elements obtained in the previous section. It has been checked that the pairs of matrix element products $V_{cb}^* V_{cb'}$ and $V_{t'b}^* V_{t'b'}$ turn in the same Jarlskog invariant $\text{Im}(V_{cb}^* V_{cb'} V_{t'b} V_{t'b'}) = +3.30 \times 10^{-6}$ but with an opposite sign. It should be the case, for the shortest side $V_{ub}^* V_{ub'}$ of the parallelogram has negligible length. We have also inspected the areas defined by the other pairs of matrix element products associated with fourth generation quarks, and affirmed that the one in Eq. (32) is the maximum. As already stated, substituting a c (s) quark for the t (b) quark in Fig. 2(b) causes suppression by the c (s) quark Yukawa coupling. Hence, the transition $t' \rightarrow b' \rightarrow t \rightarrow b \rightarrow t'$ described in Fig. 2(b) indeed captures the leading CPV source.

Note that the Jarlskog invariant for the 4×4 CKM matrix in Eq. (32) is negative. To guarantee a positive Λ^2 in Eq. (9), we must relate the sign s_f to the third component I_{3f} of the fermion f , $s_f = 2I_{3f}$ (I_{3f} has the magnitude of $1/2$). The relation accords with the choice $s_t = +1$ ($s_\tau = -1$) for the top-sourced (τ -sourced) operator in [34] inferred by the observed BAU. It is worth emphasizing that the sign s_f is not a fitting parameter, but can be specified in our formalism. Equation (9) then sets the new physics scale

$$\Lambda = \frac{64\pi^2 v^3}{g_t \sqrt{-c_J \Lambda_s^2}}, \quad (33)$$

manifesting that Λ is independent of the flavor f , contrary to the treatment in [34, 64].

Equation (33) requires the knowledge of the symmetry restoration scale Λ_s for estimating the new physics scale Λ , which can be determined in a RG analysis on the relevant Yukawa couplings. Though the evolutions of the Yukawa couplings have been probed in [11], the exact scale for the symmetry restoration remains unaddressed in the SM4. It was shown [9] that fourth generation quarks with order-of-TeV masses form bound states at a low scale, and that the heavy bound states couple to Higgs bosons weakly. This is the reason why heavy fourth generation quarks bypass the experimental constraint from Higgs production via gluon fusion. It means that heavy quark effects ought to be excluded, when the RG equations are solved around the electroweak scale. Heavy quarks, as physical degrees of freedom at a high scale, contribute to the RG evolution above the restoration scale. Such a two-stage RG study was not made in [11]; the purpose of [11] is to explore the Yukawa couplings of fourth generation quarks around the UV

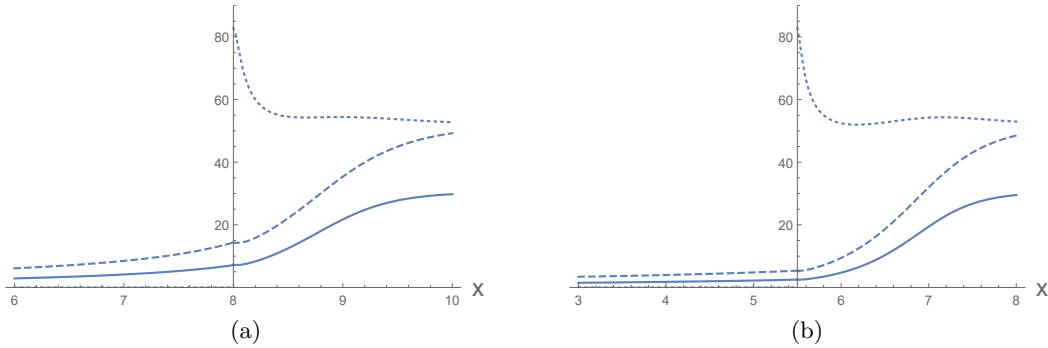


FIG. 4: Matching of RG evolutions of the Yukawa couplings g_Q^2 (dotted), g_L^2 (dashed) and g_t^2 (solid) at (a) $x_s = 8.0$ and (b) $x_s = 5.5$.

fixed point, and to certify that they are below the critical values for establishing condensates, and the electroweak symmetric phase exists at a high energy in the SM4.

We pinpoint the restoration scale Λ_s in the SM4 by solving the RG equations for the Yukawa couplings in two regions of the evolution variable $x \equiv \ln(\mu/m_Z)$ [13], μ being a renormalization scale and m_Z being the Z boson mass. In the first region x runs from $x = 0$, corresponding to the electroweak scale, i.e., the starting point of the RG evolution, to some value $x = x_s$. We switch off the heavy quark contributions in this region with $0 \leq x < x_s$. Note that the degeneracy of the fourth generation masses was assumed in the derivation of the RG equations in [13]. We set the initial condition of the heavy lepton Yukawa coupling g_L at $x = 0$ to $g_{\tau'} = \sqrt{2}m_{\tau'}/v = 1.6$ of τ' leptons for illustration. We have assured that the above simplification does not affect the outcome much. The initial condition of the t quark Yukawa coupling takes $g_t = 1.0$ at $x = 0$. In the second region x runs from $x = x_s$ to a sufficiently large value, say, $x = 12$, which has reached the UV fixed point. The heavy quark Yukawa coupling g_Q is taken into account in this region, and chosen as the critical value $g_Q^c = 9.1$ at $x = x_s$ [11]. We then adjust x_s , such that the Yukawa couplings g_L and g_t from the two regions match at $x = x_s$ smoothly. Once x_s is identified, we read off the restoration scale $\Lambda_s = m_Z \exp(z_s)$.

The matchings of the Yukawa coupling squared g_L^2 and g_t^2 at $x = x_s = 8.0$ are displayed in Fig. 4(a) to reveal the jagged transition of the RG evolutions from $x < x_s$ to $x > x_s$. Looking at the behaviors around $x = 8.0$ closely, one finds that the curves go down and up in the interval $8.0 < x < 8.3$. The matching becomes smooth as x_s decreases to a value between $x_s = 6.0$ and $x_s = 5.0$, so the assignment $x_s = 5.5$ is reasonable, for which the RG evolutions of g_Q^2 , g_L^2 and g_t^2 are shown in Fig. 4(b). It is seen that g_L^2 and g_t^2 ascend with x monotonically in the first region. In the second region g_Q^2 runs from its critical value $g_Q^c = 83$ [11] down to the fixed-point value, approaching $g_Q^{f2} = 52$ at a high x [13], the same as observed in [11]. The curves of g_L^2 and g_t^2 in the two regions meet smoothly at $x = 5.5$ with the magnitudes $g_L^2 = 5.4$ and $g_t^2 = 2.5$, respectively. The significant enhancement of the slopes at $x > x_s$ originates from the inclusion of the heavy quark effects. The curve of g_L^2 merges with that of g_Q^2 , and also approaches the fixed-point value $g_L^{f2} = 52$ at a high x . The top quark Yukawa coupling squared takes the fixed-point value $g_t^{f2} = 30$. Figure 4(b) designates the restoration scale $\Lambda_s = m_Z \exp(z_s) \approx 22$ TeV for $m_Z = 91.2$ GeV [59], in agreement with the order-of-magnitude estimate in the dispersive analysis on the lepton mixing [4].

As elaborated before, the effective operators are matched to the full theory near the restoration scale Λ_s . We then deduce, from Eq. (33) for $g_t = \sqrt{2.5}$ at $x = x_s = 5.5$ and $v = 246$ GeV,

$$\Lambda \approx 16 \text{ TeV}, \quad (34)$$

which is above the lower bounds $\Lambda_t = 7.1$ ($\Lambda_{\tau} = 1.0$) TeV for t quarks (τ leptons) from the electron EDM data[34]. A looser bound $\Lambda_{\tau} < 3.6$ TeV was concluded in [39] for the τ lepton operator to accommodate the observed BAU, which is still below Eq. (34). A more stringent constraint from the electron EDM based on the assumption of Minimal Flavor Violation, $\Lambda_{\tau} > 6$ TeV, was imposed [40]. Anyway, it is quite certain that the BAU sourced by τ leptons is insufficient in the SM4. Therefore, we turn to the BAU sourced by fourth generation leptons.

Following Eq. (14) in [34], we can construct the transport equations for the net number densities of left-handed fourth generation leptons, $L = n_{\nu'_L} + n_{\tau'_L}$, and of right-handed fourth generation leptons, $n_{\nu'_R}$ and $n_{\tau'_R}$. A net number density is defined as the difference between particle and antiparticle number densities. The ν' mass $m_4 \approx 170$ GeV is as large as the top quark mass m_t , so both the ν'_L and ν'_R net number densities are relevant. The equations are similar to those for the third generation leptons, $l = n_{\nu_L} + n_{\tau_L}$, n_{ν_R} and n_{τ_R} , respectively. We put aside the potential quark-lepton interactions as done in Sections 3 and 4 of [34]. The source terms appearing in the transport equations

sensitively depend on the methods for their derivations [65], such as the VEV-insertion approximation (VIA) [47] and the WKB expansion [66–68]; the VIA could lead to a baryon asymmetry orders of magnitude greater than the WKB formalism. Namely, tremendous theoretical uncertainties in predictions for the BAU are unavoidable, and an adequate estimation serves the purpose. It has been surveyed [34] that the predicted baryon asymmetries in the above two approaches differ by a factor of 0.2–5, varying with the flavors responsible for the source terms. The VIA method was picked up in [34].

The coupled transport equations for various net number densities of quarks and leptons have been solved in [34] with a plane bubble wall located at $z = 0$, the symmetric phase in the $z < 0$ region, and the broken phase in the $z > 0$ region. The distinction between the transport equations for lepton and quark number densities mainly arises from strong sphaleron interactions. Strong sphalerons tend to wash out the chiral asymmetry in quark, instead of lepton, number densities generated during plasma particle collisions with bubble walls and diffusing into the symmetric phase [69, 70]. As depicted in Fig. 2 of [34], the net number density l of left-handed third generation leptons plateaus at a large distance from a bubble wall due to the absence of strong sphaleron effects. It stays constant roughly at $-z > 0$ till a distance of order of the diffusion length. It is expected that the solutions for the τ'_L and ν'_L net number densities also plateau at finite $-z$, and start to descend at a distance characterized by the lepton diffusion length. That is, both the τ'_L and ν'_L net number densities behave like l , whose analytical expression has been approximated by Eq. (26) in [34]. The net number density l is negative, a consequence directly related to the sign of the CPV source. As a contrast, quark net number densities drop quickly with $-z$ in Fig. 2 of [34], signifying shorter quark diffusion lengths. A quark net number density would exhibit a feature similar to that of a lepton net number density, if there were no strong sphalerons.

Weak sphaleron effects with slow rates apply after the transport equations are solved according to the two-step process [34]. In principle, the reduction of left-handed quark net number densities by weak sphalerons makes an excess of right-handed quark net number densities in front of bubble walls, which is then absorbed by expanding bubbles, giving rise to the baryon asymmetry in the broken phase. The chiral asymmetry (or equivalently, CP asymmetries) in net number densities is turned into the baryon asymmetry through this mechanism. Nevertheless, the quark sourced chiral asymmetry would be fast redistributed between left- and right-handed quarks by strong sphalerons as reiterated before, and not efficient. Lepton chiral asymmetries are barely redistributed by strong sphalerons, and not washed out. It has been stressed that the left-handed lepton net number densities are negative. Since weak sphalerons preserve the number difference $B - L$ between left-handed baryons and leptons, the reduction of left-handed lepton net number densities creates an excess of quark net number densities. For a formulation of the baryon asymmetry as a result of weak sphaleron effects on lepton net number densities, refer to Appendix B of [34]. More details can be looked up in [71, 72].

It has been admitted that the CPV from the top quark source cannot account for the observed BAU [34]. The numerical analysis in [34] for a set of benchmark parameters discloses that top quarks contribute only about 1% of the baryon-over-entropy ratio η_B , i.e., $\eta_B^{(t)} \approx 1.6 \times 10^{-12}$ (see Table 3 and Fig. 2 in [34]). The contributions from lighter quarks, such as b quarks, are even lesser. Light neutrino contributions are also negligible, and light right-handed neutrinos decouple because of their tiny masses and Yukawa couplings. On the contrary, τ leptons, which have a finite Yukawa coupling and do not suffer the strong sphaleron suppression, play a more crucial role [37]; they induce the BAU $\eta_B = 8.2 \times 10^{-11}$ at the correct order of magnitude for the new physics scale $\Lambda_\tau = 1$ TeV and the same set of benchmark parameters in [34]. We have pointed out that the scale $\Lambda_\tau = 1$ TeV solely from the experimental constraint may be underestimated, and that the new physics scale associated with τ leptons in the SM4 is much higher.

We postulate that fourth generation leptons in the SM4, substituting for τ leptons [34], produce the observed BAU. We need not solve the coupled transport equations specific to the SM4, but extract the predictions from the framework developed by [34] based on the effective theory. Given the analytical solution in Eq. (26) of [34], the baryon-over-entropy ratio in Eq. (28) of [34] scales with the strength of the CPV source,

$$\eta_B \propto \frac{y_f}{\Lambda^2}, \quad (35)$$

as indicated in Eq. (33) of [34]. The benchmark parameters listed in Table 2 of [34] justifies the above scaling law. We take the same set of benchmark parameters as in [34], assuming the roughly equal relaxation rates, Yukawa rates, i.e., equal diffusion length and interaction length for τ'_L and ν'_L , such that their contributions to the BAU are described by the scaling law in Eq. (35).

The entries in Table 1 of [34], i.e., the predicted $\eta_B = (7.3\text{--}8.3) \times 10^{-11}$, come from the numerical solutions to the transport equations with the τ lepton source for the Yukawa coupling $g_\tau = 0.01$ and the new physics scale $\Lambda_\tau = 1.0$ TeV. Both left-handed leptons τ'_L and ν'_L contribute to the BAU in our setup. The ratio of the CPV strengths

$$\frac{(g_\tau + g_{\nu'})/\Lambda^2}{g_\tau/\Lambda_\tau^2} \approx 1, \quad (36)$$

then implies the similar outcome $\eta_B \approx 10^{-10}$ in the SM4. We do not intend to present a precise number, considering the potential large uncertainties from, for instance, the estimate of the CPV sources, the determination of the symmetry restoration scale, the variation of involved length scales, the calculations of the bubble wall velocity during the first-order phase transition [73], etc. The measurements of cosmic microwave background anisotropies and Big Bang nucleosynthesis have inferred [74–76]

$$\eta_B = (8.8 \pm 0.6) \times 10^{-11}. \quad (37)$$

We thus claim that the observed BAU can be realized in the SM4 with reasonable inputs of parameters.

V. CONCLUSION

We have continued our endeavors to investigate the important dynamics inherent in the SM4 from various experimental and theoretical aspects. The SM4 with the specific fermion mass hierarchy survives the current experimental bounds [9, 10], breaks the electroweak symmetry by means of heavy fermion condensates [77–79], achieves the first-order EWPT [80–82] through additional interactions between Higgs bosons and bound-state scalars of fourth generation quarks [11], and offers a viable CPV source for the BAU [83]. We then further demonstrated quantitatively that the prediction for the BAU sourced by fourth generation leptons accommodates the observed baryon-over-entropy ratio η_B . Instead of engaging the cumbersome bubble and transport dynamics imbedded in the first-order EWPT, we resorted to the effective theory approach which has been thoroughly studied, constructing the dimension-6 effective operators induced by fourth generation quarks with the CPV source from the 4×4 CKM matrix. The CPV strength was shown to be proportional to the Yukawa couplings of fermions involved in the effective operators. The necessary inputs of the fourth generation fermion masses and the 4×4 CKM matrix elements were obtained in the dispersive analyses on heavy quark decays and neutral quark state mixing. It is the reason why the signs and the CPV strengths of the effective operators could be fixed unambiguously in our formalism.

It has been argued that the transport equations for fourth generations leptons are similar to those for third generation leptons, if the same relaxation rates and Yukawa rates were assumed. The solutions for their net number densities then share the similar behavior, and their contributions to the BAU are proportional to the CPV strengths of the corresponding effective operators. Hence, it is straightforward to extract the predictions for the BAU, given the same benchmark parameters, by scaling the τ lepton sourced results available in the literature. The τ sourced BAU in our SM4 setup is down by the new physics scale specified via the RG evolutions of the Yukawa couplings. The role of the τ source is replaced by the τ' and ν' sources, and the predicted ratio $\eta_B \approx 10^{-10}$ is in consistency with the observed value. Our series of works manifests that fourth generation quarks play the major role (through their condensates and bound states) for accomplishing the electroweak symmetry breaking and the first-order EWPT, while fourth generation leptons with the CPV source from the 4×4 CKM matrix are responsible for the realization of the BAU.

We have also taken this chance to revisit the dispersive constraints on the neutrino masses and the PMNS matrix elements in the presence of fourth generation leptons. It was found that a heavy fourth generation demands the almost exact unitarity of the 3×3 PMNS matrix. Solving the dispersive constraints in an alternative way, we corroborate that the known inputs of the mass-squared differences Δm_{21}^2 and Δm_{32}^2 lead to the mixing angles and CP phase in the 3×3 PMNS matrix $\theta_{12} \approx 34^\circ$, $\theta_{23} \approx 47^\circ$, $\theta_{13} \approx 5^\circ$ and $\delta \approx 200^\circ$. These results are insensitive to the variation of the lightest neutrino mass m_1 , and close to the data for the normal ordering scenario. The distinct mixing patterns in the quark and lepton sectors is attributed to the different quark and lepton mass spectra. The angle θ_{23} is preferred to be in the second octant. The consistencies of our SM4 setup in various aspects encourage the search for heavy fourth generation fermions at the (high-luminosity) large hadron collider or a muon collider.

Appendix A: Pseudoscalar Penguin

We construct the pseudoscalar penguin operator, which will facilitate the derivation of the dimension-6 effective operator with a CPV source. The computation is similar to that in [84], where a heavy vector quark is integrated out to produce effective operators in terms of SM fields. The Feynman rules for charged-scalar-quark vertices in the R_ξ gauge with $\xi = 0$ are written as

$$iV_{ud}^* \left(g_u \frac{1 + \gamma_5}{2} - g_d \frac{1 - \gamma_5}{2} \right), \quad iV_{ud} \left(g_u \frac{1 - \gamma_5}{2} - g_d \frac{1 + \gamma_5}{2} \right), \quad (A1)$$

for an incoming up-type quark and an outgoing down-type quark, and for an incoming down-type quark and an outgoing up-type quark, respectively, where V_{ud} is the corresponding CKM matrix element, and g_u (g_d) is the Yukawa

coupling of the up-type (down-type) quark. The pseudoscalar-fermion vertex reads

$$-\sqrt{2}g_f I_{3f} \gamma_5, \quad (\text{A2})$$

I_{3f} being the third component of the fermion isospin.

Figure 3 contains the relevant diagrams for the $t' \rightarrow t$ transition, where the incoming t' (outgoing t) quark carries the momentum p_1 (p_2). The vertex correction in Fig. 3(a) consists of a charged scalar loop with a pseudoscalar boson attaching the internal b' quark line. It gives the loop integral

$$\begin{aligned} P_V = & -\sqrt{2}V_{t'b'}^* V_{tb'} g_{b'} I_{3b'} \int \frac{d^4 l}{(2\pi)^4} \left(-ig_{b'} \frac{1 + \gamma_5}{2} \right) \frac{i(\not{p}_2 - \not{l} + m_{b'})}{(p_2 - l)^2 - m_{b'}^2} \gamma_5 \\ & \times \frac{i(\not{p}_1 - \not{l} + m_{b'})}{(p_1 - l)^2 - m_{b'}^2} i \left(g_{t'} \frac{1 + \gamma_5}{2} - g_{b'} \frac{1 - \gamma_5}{2} \right) \frac{i}{l^2}. \end{aligned} \quad (\text{A3})$$

We keep only the dominant term $g_{t'}(1 + \gamma_5)/2$ in the parentheses in Eq. (A3) because of $g_{t'} > g_{b'}$, arriving at

$$P_V = -\frac{i}{\sqrt{2}} V_{t'b'}^* V_{tb'} I_{3b'} g_{b'}^2 g_{t'} \int \frac{d^4 l}{(2\pi)^4} \frac{(\not{p}_2 - \not{l})(\not{p}_1 - \not{l}) - m_{b'}^2}{[(p_2 - l)^2 - m_{b'}^2][(p_1 - l)^2 - m_{b'}^2]l^2} (1 + \gamma_5). \quad (\text{A4})$$

The numerator can be organized into

$$(\not{p}_2 - \not{l})(\not{p}_1 - \not{l}) - m_{b'}^2 = (\not{p}_1 - \not{l} - \not{q})(\not{p}_1 - \not{l}) = [(p_1 - l)^2 - m_{b'}^2] - \not{q}(\not{p}_1 - \not{l}), \quad (\text{A5})$$

with the momentum transfer $q = p_1 - p_2$. The first term $(p_1 - l)^2 - m_{b'}^2$ cancels the one in the denominator, yielding

$$-\frac{i}{\sqrt{2}} V_{t'b'}^* V_{tb'} I_{3b'} g_{b'}^2 g_{t'} \int \frac{d^4 l}{(2\pi)^4} \frac{1 + \gamma_5}{[(p_2 - l)^2 - m_{b'}^2]l^2}. \quad (\text{A6})$$

The self-energy correction associated with the $t' \rightarrow t$ transition in Fig 3(b) is written as

$$P_S = -\sqrt{2}V_{t'b'}^* V_{tb'} g_{t'} I_{3t'} \int \frac{d^4 l}{(2\pi)^4} \left(-ig_{b'} \frac{1 + \gamma_5}{2} \right) \frac{i(\not{p}_2 - \not{l} + m_{b'})}{(p_2 - l)^2 - m_{b'}^2} \left(ig_{t'} \frac{1 + \gamma_5}{2} \right) \frac{i(\not{p}_2 + m_{t'})}{p_2^2 - m_{t'}^2} \gamma_5 \frac{i}{l^2}. \quad (\text{A7})$$

To simplify the calculation and grasp the important contribution, we drop p_2 relative to the largest mass $m_{t'}$, attaining

$$\begin{aligned} P_S = & -\sqrt{2}V_{t'b'}^* V_{tb'} g_{t'} I_{3t'} \frac{-ig_{b'} g_{t'}}{2} \int \frac{d^4 l}{(2\pi)^4} \frac{m_{b'}}{[(p_2 - l)^2 - m_{b'}^2]l^2} (1 + \gamma_5) \frac{-1}{m_{t'}} \gamma_5 \\ = & -\frac{i}{\sqrt{2}} V_{t'b'}^* V_{tb'} I_{3t'} g_{b'}^2 g_{t'} \int \frac{d^4 l}{(2\pi)^4} \frac{1 + \gamma_5}{[(p_2 - l)^2 - m_{b'}^2]l^2}. \end{aligned} \quad (\text{A8})$$

The above integral is identical to Eq. (A6) except the isospin component $I_{3t'} = -I_{3b'}$, so they cancel each other exactly. It indicates that the pseudoscalar penguin is UV finite, and the difference between the vertex and self-energy corrections diminishes as $q \rightarrow 0$.

We turn to the net contribution from the second term on the right-hand side of Eq. (A5). The numerator becomes, after the variable change $l \rightarrow l + xp_1 + yp_2$ and the Feynman parametrization,

$$-\not{q}(\not{p}_1 - \not{l}) \rightarrow x \not{q} \not{p}_1 - q^2, \quad (\text{A9})$$

where the term linear in the loop momentum l has been removed. The first term, leading to an integrand with an odd power of the loop momentum in Fig. 2(b), does not contribute. Note that the momentum p_1 will be treated as a loop momentum in the evaluation of Fig. 2(b). Equation (A9) then appears in the desired form; the factor q^2 cancels the propagator of the virtual pseudoscalar, which is proportional to $1/q^2$, producing a local operator. The Feynman parametrization recasts the denominator into

$$\begin{aligned} & l^2 - (xp_1 + yp_2)^2 + x(p_1^2 - m_{b'}^2) + y(p_2^2 - m_{b'}^2) \\ = & l^2 + x(1 - x - y)p_1^2 + y(1 - x - y)p_2^2 - (x + y)m_{b'}^2 + xyq^2. \end{aligned} \quad (\text{A10})$$

The loop integral is dominated by the configuration, where the momentum p_1 is roughly on-shell with $p_1^2 \approx m_{b'}^2$, and splits into p_2 and q with smaller invariants p_2^2 and q^2 . Equation (A10) is thus approximated by

$$l^2 - [(1 + x)(x + y) - x]m_{b'}^2. \quad (\text{A11})$$

We have the sum

$$\begin{aligned} P_V + P_S &= -\frac{i}{\sqrt{2}} V_{t'b'}^* V_{tb'} I_{3b'} g_{b'}^2 g_{t'} \int_0^1 dx \int_0^{1-x} dy \int \frac{d^4 l}{(2\pi)^4} \frac{-q^2(1+\gamma_5)}{\{l^2 - [(1+x)(x+y)-x]m_{b'}^2\}^3} \\ &= \frac{1}{192\sqrt{2}} V_{t'b'}^* V_{tb'} I_{3b'} g_{b'}^2 g_{t'} \frac{q^2}{m_{b'}^2} (1+\gamma_5). \end{aligned} \quad (\text{A12})$$

At last, we multiply the above expression by the virtual pseudoscalar propagator and the spinors of the initial- and final-state fermions, establishing the four-fermion operator

$$\begin{aligned} P &= \frac{1}{192\sqrt{2}} V_{t'b'}^* V_{tb'} I_{3b'} g_{b'}^2 g_{t'} \frac{q^2}{m_{b'}^2} \bar{t}(1+\gamma_5) t' \frac{i}{q^2} (-\sqrt{2} g_f I_{3f}) \bar{f} \gamma_5 f \\ &= -\frac{i}{192} V_{t'b'}^* V_{tb'} I_{3b'} I_{3f} \frac{g_f g_{b'}^2 g_{t'}}{m_{b'}^2} \bar{t}(1+\gamma_5) t' \bar{f} \gamma_5 f. \end{aligned} \quad (\text{A13})$$

It is learned that the pseudoscalar penguin can be constructed in the heavy quark limit, similar to the penguin operators in the conventional effective weak Hamiltonian. We emphasize that the above derivation does not apply, as the virtual pseudoscalar is replaced by a virtual scalar. In this case the mass squared term in Eq. (A4) would flip sign, such that one cannot have the exact cancellation of the q -independent pieces between the vertex and self-energy corrections.

It is trivial to obtain the self-energy correction associated with the $t \rightarrow t'$ transition,

$$\begin{aligned} S &= V_{tb}^* V_{t'b} \int \frac{d^4 l}{(2\pi)^4} i g_{t'} \frac{1-\gamma_5}{2} \frac{i(\not{p}-\not{l})}{(p-l)^2} i g_t \frac{1+\gamma_5}{2} \frac{i}{l^2} \\ &= \frac{i}{64\pi^2} V_{tb}^* V_{t'b} g_{t'} g_t \left(\ln \frac{\Lambda_s^2}{-p^2} + 1 \right) \not{p} (1+\gamma_5), \end{aligned} \quad (\text{A14})$$

with the t quark momentum p . Because the full theory holds up to the electroweak symmetry restoration scale, we have bounded the loop momentum at Λ_s .

Appendix B: DISPERSIVE CONSTRAINTS ON THE 4×4 PMNS MATRIX

We review the dispersive constraints on the 4×4 PMNS matrix, which were extracted from the mixing amplitudes associated with the neutral lepton pairs $\mathcal{L}^-\ell^+$ and $\mathcal{L}^+\ell^-$ [10], \mathcal{L} (ℓ) being a massive (light) lepton. Our discussion covers the μe and τe systems specifically, but not the $\tau\mu$ mixing; the mass ratio $m_\tau/m_\mu \sim O(10)$, much lower than $m_t/m_c \sim O(100)$, hints that the present formalism for a heavy-light system may not work for the $\tau\mu$ mixing. The tc mixing was considered in Sec. III. It is not necessary to touch the $\tau'e$ mixing, because we have known that $U_{\tau'1}$, $U_{\tau'2}$ and $U_{\tau'3}$ diminish and $U_{\tau'4} \approx 1$ in the fourth row of the PMNS matrix. We will solve the dispersive constraints in a manner different from that in [10]. The same conclusion drawn in this appendix verifies the validity of the approximate solutions in [10]. Besides, the formalism presented here applies to the 4×4 CKM matrix for the quark mixing in Sec. III straightforwardly.

We decompose the mixing amplitude $\Pi(m_{\mathcal{L}}^2)$ into a sum over intermediate neutrino channels,

$$\begin{aligned} \Pi(m_{\mathcal{L}}^2) &= M(m_{\mathcal{L}}^2) - \frac{i}{2} \Gamma(m_{\mathcal{L}}^2) \\ &\equiv \sum_{i,j=1}^4 \lambda_i \lambda_j \left[M_{ij}(m_{\mathcal{L}}^2) - \frac{i}{2} \Gamma_{ij}(m_{\mathcal{L}}^2) \right], \end{aligned} \quad (\text{B1})$$

where $\lambda_i \equiv U_{\mathcal{L}i}^* U_{\ell i}$ is the product of the 4×4 PMNS matrix elements with i referring to the i -th generation neutrino. It has been illustrated that the electroweak symmetry is restored above a scale Λ_s in our SM4 setup [11], and that the mixing phenomenon disappears as $m_{\mathcal{L}} > \Lambda_s$; all internal particles become massless in the symmetric phase, such that the summation over all intermediate channels is strongly suppressed by the unitarity of the PMNS matrix. Small finite contributions to the real part $M_{ij}(m_{\mathcal{L}}^2)$ begin only at the three-loop level in the symmetric phase [4]. The corresponding dispersion relation is thus expressed as

$$M(m_{\mathcal{L}}^2) = \frac{1}{2\pi} \int_{m_{\mathcal{L}}^2}^{\Lambda_s^2} dm^2 \frac{\Gamma(m^2)}{m_{\mathcal{L}}^2 - m^2} \approx 0, \quad (\text{B2})$$

for $m_{\mathcal{L}} > \Lambda_s$, where the upper bound of the integration variable m^2 is set to Λ_s^2 .

To obey Eq. (B2) for arbitrary $m_{\mathcal{L}} > \Lambda_s$, some conditions must be met by the PMNS matrix elements appearing in the imaginary part $\Gamma(m^2)$. We quote the asymptotic behavior of the component $\Gamma_{ij}(m^2)$ for $m < \Lambda_s$ [85, 86]

$$\Gamma_{ij}(m^2) \approx \Gamma_{ij}^{(1)} m^2 + \Gamma_{ij}^{(0)} + \frac{\Gamma_{ij}^{(-1)}}{m^2} + \dots, \quad (B3)$$

where the coefficients $\Gamma_{ij}^{(n)}$, $n = 1, 0, -1$, have been presented in [10]. These terms give contributions to the dispersive integral in Eq. (B2), which scale like Λ_s^4 , Λ_s^2 and $\ln \Lambda_s^2$ for $n = 1, 0$ and -1 , respectively. Since the upper bound Λ_s represents an order-of-magnitude concept, instead of a definite value, it is unlikely that the above huge contributions happen to cancel among themselves. Therefore, the finiteness of the dispersive integral must be fulfilled by vanishing the sum of the coefficients

$$\sum_{i,j=1}^4 \lambda_i \lambda_j \Gamma_{ij}^{(n)} \approx 0, \quad n = 1, 0, -1. \quad (B4)$$

Once the conditions in Eq. (B4) are conformed, we rewrite the dispersive integral in Eq. (B2) as

$$\int_{t_{ij}}^{\Lambda_s^2} dm^2 \frac{\Gamma(m^2)}{m_{\mathcal{L}}^2 - m^2} \approx \frac{1}{m_{\mathcal{L}}^2} \sum_{i,j=1}^4 \lambda_i \lambda_j g_{ij}, \quad (B5)$$

with the factors

$$g_{ij} \equiv \int_{t_{ij}}^{\infty} dm^2 \left[\Gamma_{ij}(m^2) - \Gamma_{ij}^{(1)} m^2 - \Gamma_{ij}^{(0)} - \frac{\Gamma_{ij}^{(-1)}}{m^2} \right], \quad (B6)$$

$t_{ij} = (m_i + m_j)^2$ being the threshold for one of the channel. The integrand in the square brackets decreases like $1/m^4$, so the upper bound of m^2 in Eq. (B6) can be pushed to infinity safely. The approximation $1/(m_{\mathcal{L}}^2 - m^2) \approx 1/m_{\mathcal{L}}^2$ has been made for large $m_{\mathcal{L}} > \Lambda_s$, because the integral receives contributions only from finite $m < \Lambda_s$. We place the final condition,

$$\sum_{i,j=1}^4 \lambda_i \lambda_j g_{ij} \approx 0, \quad (B7)$$

to guarantee an almost nil dispersive integral. That is, Eqs. (B4) and (B7) constitute a solution to the integral equation (B2).

We eliminate $\lambda_4 = -\lambda_1 - \lambda_2 - \lambda_3$ using the unitarity condition, and define the ratios of the PMNS matrix elements,

$$r_1 \equiv \frac{U_{\mathcal{L}1}^* U_{e1}}{U_{\mathcal{L}2}^* U_{e2}} \equiv u_1 + iv_1, \quad r_3 \equiv \frac{U_{\mathcal{L}3}^* U_{e3}}{U_{\mathcal{L}2}^* U_{e2}} \equiv u_3 + iv_3, \quad (B8)$$

where \mathcal{L} stands for either μ or τ , and the unknowns $u_{1,3}$ and $v_{1,3}$ will be constrained below. The $n = 1, 0$ and -1 conditions are then formulated as [10]

$$\left(r_1 \frac{m_4^2 - m_1^2}{m_W^2 - m_1^2} + \frac{m_4^2 - m_2^2}{m_W^2 - m_2^2} + r_3 \frac{m_4^2 - m_3^2}{m_W^2 - m_3^2} \right)^2 \approx 0, \quad (B9)$$

$$\left(r_1 \frac{m_4^2 - m_1^2}{m_W^2 - m_1^2} + \frac{m_4^2 - m_2^2}{m_W^2 - m_2^2} + r_3 \frac{m_4^2 - m_3^2}{m_W^2 - m_3^2} \right) \left(r_1 \frac{m_4^2 - m_1^2}{m_W^2 - m_1^2} P_1 + \frac{m_4^2 - m_2^2}{m_W^2 - m_2^2} P_2 + r_3 \frac{m_4^2 - m_3^2}{m_W^2 - m_3^2} P_3 \right) \approx 0, \quad (B10)$$

$$\left(r_1 \frac{m_4^2 - m_1^2}{m_W^2 - m_1^2} + \frac{m_4^2 - m_2^2}{m_W^2 - m_2^2} + r_3 \frac{m_4^2 - m_3^2}{m_W^2 - m_3^2} \right) \left(r_1 \frac{m_4^2 - m_1^2}{m_W^2 - m_1^2} Q_1 + \frac{m_4^2 - m_2^2}{m_W^2 - m_2^2} Q_2 + r_3 \frac{m_4^2 - m_3^2}{m_W^2 - m_3^2} Q_3 \right) \approx 0, \quad (B11)$$

respectively, with the functions

$$\begin{aligned} P_i &= \frac{m_W^2 (m_4^2 + m_i^2) - m_4^2 m_i^2}{m_4^4} \\ Q_i &= \frac{2m_W^4 (m_4^2 + m_i^2) + m_4^2 m_i^2 (m_4^2 + m_i^2) - m_W^2 (m_4^4 + 3m_4^2 m_i^2 + m_i^4)}{m_4^6}. \end{aligned} \quad (B12)$$

The last condition in Eq. (B7) turns into [10]

$$-(20m_W^4 - 28m_W^2m_4^2 + 7m_4^4)G_0 + (16m_W^4 - 28m_4^2m_W^2 + 12m_4^4)G_1 \approx 0, \quad (\text{B13})$$

$$G_0 = \left(\frac{r_1}{m_W^2 - m_1^2} + \frac{1}{m_W^2 - m_2^2} + \frac{r_3}{m_W^2 - m_3^2} \right)^2, \quad (\text{B14})$$

$$G_1 = \left(\frac{r_1}{m_W^2 - m_1^2} + \frac{1}{m_W^2 - m_2^2} + \frac{r_3}{m_W^2 - m_3^2} \right) \left[\frac{r_1 m_1}{m_4(m_W^2 - m_1^2)} + \frac{m_2}{m_4(m_W^2 - m_2^2)} + \frac{r_3 m_3}{m_4(m_W^2 - m_3^2)} \right]. \quad (\text{B15})$$

Our alternative strategy to solve the coupled Eqs. (B9)-(B11) and (B13) is detailed as follows. We first solve for u_3 and v_3 in terms of u_1 and v_1 from the real part of Eq. (B9)

$$u_1 \frac{m_4^2 - m_1^2}{m_W^2 - m_1^2} + \frac{m_4^2 - m_2^2}{m_W^2 - m_2^2} + u_3 \frac{m_4^2 - m_3^2}{m_W^2 - m_3^2} = v_1 \frac{m_4^2 - m_1^2}{m_W^2 - m_1^2} + v_3 \frac{m_4^2 - m_3^2}{m_W^2 - m_3^2}, \quad (\text{B16})$$

and the real part of Eq.(B13). Inserting the expressions of u_3 and v_3 into the rest of constraints, we minimize the deviations of the imaginary part of Eq. (B9), both real and imaginary parts of Eq. (B10), and the imaginary part of Eq. (B13) by tuning u_1 and v_1 . The coupled equations are fully respected in this sense. The difference between Eqs. (B11) and (B10) are numerically negligible, so the former can be excluded. We assume a small first generation mass $m_1^2 = 10^{-6}$ eV² [3], and input m_2 and m_3 from the measured mass-squared differences $\Delta m_{21}^2 \equiv m_2^2 - m_1^2 = (7.50_{-0.20}) \times 10^{-5}$ eV² and $\Delta m_{31}^2 \equiv m_3^2 - m_1^2 = (2.55_{-0.03}) \times 10^{-3}$ eV² in the normal-ordering scenario [87]. It has been demonstrated [3] that the inverted mass ordering is not favored by the dispersive constraints. The above parameters were updated in [88, 89] with tiny changes, such as $\Delta m_{21}^2 = (7.55_{-0.20}) \times 10^{-5}$ eV² [88]. The fourth generation neutrino mass and the W boson mass take $m_{\nu'} = 170$ GeV and $m_W = 80.37$ GeV, respectively.

The tuning of u_1 and v_1 is proceeded in a way similar to that in [3]. We first inspect the dependencies of the aforementioned four constraints on u_1 for $v_1 = 0$. It is seen that the first three have a single root $u_1 \approx 0.97$, while the last one reveals two roots $u_1 \approx -0.97$ and $u_1 \approx -0.83$, which arise from Eq. (B15),

$$\left(\frac{u_1}{m_W^2 - m_1^2} + \frac{1}{m_W^2 - m_2^2} + \frac{u_3}{m_W^2 - m_3^2} \right) \left(u_1 \frac{m_4^2 - m_1^2}{m_W^2 - m_1^2} + \frac{m_4^2 - m_2^2}{m_W^2 - m_2^2} + u_3 \frac{m_4^2 - m_3^2}{m_W^2 - m_3^2} \right) = 0. \quad (\text{B17})$$

When Eq. (B9) is satisfied, the magnitude of Eq. (B14) diminishes, for Eqs. (B9) and (B14) differ only by $O(m_i^2/m_{4,W}^2)$. Namely, Eq. (B13) is governed by the second term, which should vanish as shown in Eq. (B17). It describes a parabola in u_1 , explaining the existence of the two roots. It is encouraging that $u_1 \approx -0.97$ and $u_1 \approx -0.83$ are close to the real parts of r_1 associated with the μe and τe mixings, respectively. To meet the four constraints for the μe and τe mixings simultaneously, v_1 , which is related to the CP phase of the PMNS matrix, must take a finite value; for a finite v_1 , the first three constraints develop an additional root of u_1 around $u_1 \approx -0.83$. We increase v_1 gradually until this additional root of u_1 coincides with the minimal deviation of the fourth condition from zero. This best-fit v_1 is found to be $v_1 \approx -0.04$, corresponding to which the two roots of u_1 shift a bit to -0.98 and -0.84 .

As pointed out in [10], v_1 is determined up to a sign; the right-hand side of Eq. (B16) can have a minus sign, which also minimizes the real part of Eq. (B9). We then obtain the solutions of r_1 for the μe and τe mixings,

$$\frac{U_{\mu 1}^* U_{e 1}}{U_{\mu 2}^* U_{e 2}} = -0.84 - 0.04i, \quad \frac{U_{\tau 1}^* U_{e 1}}{U_{\tau 2}^* U_{e 2}} = -0.98 + 0.04i, \quad (\text{B18})$$

where the sign of v_1 has been assigned appropriately. Equation (B18) is insensitive to the choices of the light neutrino mass m_1 , as long as it is sufficiently lower than m_2 . Equation (B18) is almost identical to $-0.83 - 0.04i$ and $-0.98 + 0.04i$ derived in [10]. We mention that the solutions for $r_{1,3}$ well respect the unitarity of the 3×3 PMNS matrix. This is obvious from the constraints in Eqs. (B9)-(B11) and (B13), which require $u_1 + u_3 \approx -1$ and $v_1 + v_3 \approx 0$. For example, inserting $u_1 = -0.84$ and $v_1 = -0.04$ into the expressions for u_3 and v_4 , we get $u_3 = -0.26$ and $v_3 = 0.04$.

The above formalism certainly extends to the quark mixing, such as the $c\bar{u} - \bar{c}u$ and $t\bar{u} - \bar{t}u$ mixings with d, s, b and b' quarks in the intermediate channels. The corresponding dispersive constraints are copied from those for the lepton mixing by simply substituting the quark masses m_d, m_s, m_b and $m_{b'}$ for m_1, m_2, m_3 and m_4 , respectively. As remarked in Sec. III, different solutions for the quark and lepton mixings come from the disparate mass spectra of quarks and leptons. The goal of the dispersive analysis on the 4×4 CKM matrix is to estimate the fourth column and fourth row elements, which may not diminish, and are essential for assessing the CPV strength of the dimension-6 effective operators.

Acknowledgement

We thank K.F. Chen, Y.T. Chien, C.S. Chu, S.Y. Ho, W.S. Hou, Y.J. Lin, S.M. Wang, M.R. Wu, Y.L. Wu, X.B. Yuan and X.M. Zhang for fruitful discussions. We also thank the Yukawa Institute for Theoretical Physics at Kyoto University, where part of the work was completed during “Progress of Theoretical Bootstrap”. This work was supported by National Science and Technology Council of the Republic of China under Grant No. MOST-113-2112-M-001-024-MY3.

[1] H. n. Li, Phys. Rev. D **107**, no.9, 094007 (2023).

[2] H. n. Li, Phys. Rev. D **108**, no.5, 054020 (2023).

[3] H. n. Li, [arXiv:2306.03463 [hep-ph]].

[4] H. n. Li, Chin. J. Phys. **92**, 1043-1054 (2024).

[5] G. F. Chew, Rev. Mod. Phys. **34**, no.3, 394-401 (1962).

[6] J. T. Cushing, Stud. Hist. Phil. Sci. A **16**, 31-48 (1985).

[7] R. van Leeuwen, Stud. Hist. Phil. Sci. **104** (2024), 130-149.

[8] G. F. Chew and J. Finkelstein, Phys. Rev. Lett. **50**, 795 (1983).

[9] H. n. Li, Phys. Rev. D **109**, no.11, 115024 (2024).

[10] H. n. Li, J. Phys. G **52** (2025) 025001.

[11] H. n. Li, JHEP **09** (2025), 037.

[12] W. A. Bardeen, C. T. Hill and M. Lindner, Phys. Rev. D **41** (1990) 1647.

[13] P. Q. Hung and C. Xiong, Nucl. Phys. B **847**, 160-178 (2011).

[14] T. Enkhbat, W. S. Hou and H. Yokoya, Phys. Rev. D **84**, 094013 (2011).

[15] N. Chen and H. J. He, JHEP **04**, 062 (2012); O. Eberhardt, G. Herbert, H. Lacker, A. Lenz, A. Menzel, U. Nierste and M. Wiebusch, Phys. Rev. Lett. **109**, 241802 (2012); A. Djouadi and A. Lenz, Phys. Lett. B **715**, 310-314 (2012); E. Kuflik, Y. Nir and T. Volansky, Phys. Rev. Lett. **110**, no.9, 091801 (2013).

[16] H. J. He, N. Polonsky and S. f. Su, Phys. Rev. D **64**, 053004 (2001).

[17] X. Marcano, [arXiv:2405.10840 [hep-ph]].

[18] R. Joshi and R. Roy, [arXiv:2510.25190 [hep-ph]].

[19] A. D. Sakharov, Pisma Zh. Eksp. Teor. Fiz. **5**, 32-35 (1967).

[20] G. R. Farrar and M. E. Shaposhnikov, Phys. Rev. Lett. **70**, 2833-2836 (1993) [erratum: Phys. Rev. Lett. **71**, 210 (1993)].

[21] G. R. Farrar and M. E. Shaposhnikov, Phys. Rev. D **50**, 774 (1994).

[22] M. B. Gavela, P. Hernandez, J. Orloff and O. Pene, Mod. Phys. Lett. A **9**, 795-810 (1994).

[23] M. B. Gavela, M. Lozano, J. Orloff and O. Pene, Nucl. Phys. B **430**, 345-381 (1994).

[24] M. B. Gavela, P. Hernandez, J. Orloff, O. Pene and C. Quimbay, Nucl. Phys. B **430**, 382-426 (1994).

[25] K. Kajantie, M. Laine, K. Rummukainen and M. E. Shaposhnikov, Phys. Rev. Lett. **77**, 2887-2890 (1996).

[26] K. Rummukainen, M. Tsypin, K. Kajantie, M. Laine and M. E. Shaposhnikov, Nucl. Phys. B **532**, 283-314 (1998).

[27] F. Csikor, Z. Fodor and J. Heitger, Phys. Rev. Lett. **82**, 21-24 (1999).

[28] Y. Aoki, F. Csikor, Z. Fodor and A. Ukawa, Phys. Rev. D **60**, 013001 (1999).

[29] S. R. Coleman and E. J. Weinberg, Phys. Rev. D **7** (1973) 1888-1910.

[30] L. Dolan and R. Jackiw, Phys. Rev. D **9** (1974) 3320-3341.

[31] J. van de Vis, J. de Vries and M. Postma, [arXiv:2508.09989 [hep-ph]].

[32] G. Barni, [arXiv:2510.21915 [hep-ph]].

[33] C. Balazs, G. White and J. Yue, JHEP **03** (2017), 030.

[34] J. De Vries, M. Postma and J. van de Vis, JHEP **04** (2019), 024.

[35] X. Zhang, S. K. Lee, K. Whisnant and B. L. Young, Phys. Rev. D **50** (1994), 7042-7047.

[36] M. Joyce, T. Prokopec and N. Turok, Phys. Lett. B **338**, 269-275 (1994).

[37] D. J. H. Chung, B. Garbrecht, M. J. Ramsey-Musolf and S. Tulin, Phys. Rev. D **81** (2010), 063506.

[38] D. J. H. Chung, B. Garbrecht, M. J. Ramsey-Musolf and S. Tulin, Phys. Rev. Lett. **102**, 061301 (2009).

[39] E. Fuchs, M. Losada, Y. Nir and Y. Viernik, JHEP **05**, 056 (2020).

[40] J. Alonso-González, L. Merlo and S. Pokorski, JHEP **06**, 166 (2021).

[41] Y. Z. Li, M. J. Ramsey-Musolf and J. H. Yu, [arXiv:2404.19197 [hep-ph]].

[42] H. Liu and L. Bian, [arXiv:2512.16537 [hep-ph]].

[43] D. Bodeker, L. Fromme, S. J. Huber and M. Seniuch, JHEP **02** (2005), 026.

[44] L. Fromme and S. J. Huber, JHEP **03** (2007), 049.

[45] A. B. Beneito, I. A. Palavrić and A. Sainaghi, [arXiv:2512.14813 [hep-ph]].

[46] N. Košnik, A. Palavrić and A. Smolković, Phys. Rev. D **112** (2025) no.9, 095046.

[47] C. Lee, V. Cirigliano and M. J. Ramsey-Musolf, Phys. Rev. D **71** (2005), 075010.

[48] F. P. Huang, P. H. Gu, P. F. Yin, Z. H. Yu and X. Zhang, Phys. Rev. D **93** (2016) no.10, 103515.

[49] J. de Vries, M. Postma, J. van de Vis and G. White, JHEP **01** (2018), 089.

[50] C. Jarlskog, Phys. Rev. Lett. **55** (1985) 1039.

[51] C. Jarlskog, Z. Phys. C **29** (1985) 491-497.

[52] M. E. Shaposhnikov, JETP Lett. **44** (1986) 465-468.

[53] L. Silvestrini, [arXiv:1905.00798 [hep-ph]].

[54] H. n. Li, H. Umeeda, F. Xu and F. S. Yu, Phys. Lett. B **810**, 135802 (2020).

[55] H. n. Li, Phys. Rev. D **107**, no.5, 054023 (2023).

[56] Y. T. Chien and H. n. Li, Phys. Rev. D **97**, no.5, 053006 (2018).

[57] A. K. Alok, A. Dighe and D. London, Phys. Rev. D **83**, 073008 (2011).

[58] Y. H. Ahn, H. Y. Cheng and S. Oh, Phys. Lett. B **703**, 571-575 (2011).

[59] S. Navas et al. (Particle Data Group), Phys. Rev. D **110**, 030001 (2024).

[60] G. Kaur, G. Ahuja, D. Shukla and M. Gupta, Int. J. Mod. Phys. A **39** (2024) no.25, 2450102.

[61] T. Kitahara, Int. J. Mod. Phys. A **39** (2024) no.26n27, 2442011.

[62] M. Gorchtein, V. Katyal, B. Ohayon, B. K. Sahoo and C. Y. Seng, Phys. Rev. Res. **7** (2025) no.4, 4.

[63] C. Y. Seng, Mod. Phys. Lett. A **37**, no.02, 2230002 (2022).

[64] S. J. Huber, M. Pospelov and A. Ritz, Phys. Rev. D **75**, 036006 (2007).

[65] J. M. Cline and B. Laurent, Phys. Rev. D **104** (2021) no.8, 083507.

[66] M. Joyce, T. Prokopec and N. Turok, Phys. Rev. Lett. **75** (1995), 1695-1698 [erratum: Phys. Rev. Lett. **75** (1995), 3375].

[67] J. M. Cline, M. Joyce and K. Kainulainen, JHEP **07** (2000), 018.

[68] J. M. Cline, Phil. Trans. Roy. Soc. Lond. A376, 20170116 (2018), [arXiv:1704.08911 [hep-ph]].

[69] R. N. Mohapatra and X. m. Zhang, Phys. Rev. D **45** (1992), 2699-2705.

[70] G. F. Giudice and M. E. Shaposhnikov, Phys. Lett. B **326** (1994), 118-124.

[71] E. Fuchs, M. Losada, Y. Nir and Y. Viernik, JHEP **07** (2021), 060.

[72] M. Joyce, T. Prokopec and N. Turok, Phys. Rev. D **53** (1996), 2930-2957.

[73] J. van de Vis, P. Schicho, L. Niemi, B. Laurent, J. Hirvonen and O. Gould, [arXiv:2510.27691 [hep-ph]].

[74] C. L. Bennett et al. [WMAP], Astrophys. J. **583** (2003), 1-23.

[75] N. Aghanim et al. [Planck], Astron. Astrophys. **641** (2020), A6 [erratum: Astron. Astrophys. **652** (2021), C4].

[76] B. D. Fields, K. A. Olive, T. H. Yeh and C. Young, JCAP **03** (2020), 010 [erratum: JCAP **11** (2020), E02].

[77] B. Holdom, Phys. Rev. Lett. **57**, 2496 (1986), [Erratum-ibid. 58, 177 (1987)]; W. A. Bardeen, C. T. Hill and M. Lindner, Phys. Rev. D **41**, 1647 (1990); C. T. Hill, M. A. Luty and E. A. Paschos, Phys. Rev. D **43**, 3011 (1991); T. Elliott and S. F. King, Phys. Lett. B **283**, 371 (1992).

[78] P. Q. Hung and C. Xiong, Nucl. Phys. B **848** (2011) 288-302.

[79] Y. Mimura, W. S. Hou and H. Kohyama, JHEP **11**, 048 (2013).

[80] S. W. Ham, S. K. Oh and D. Son, Phys. Rev. D **71**, 015001 (2005); M. S. Carena, A. Megevand, M. Quiros and C. E. M. Wagner, Nucl. Phys. B **716**, 319 (2005).

[81] R. Fok and G. D. Kribs, Phys. Rev. D **78** (2008) 075023.

[82] Y. Kikukawa, M. Kohda and J. Yasuda, Prog. Theor. Phys. **122** (2009) 401-426.

[83] W. S. Hou, Chin. J. Phys. **47**, 134 (2009).

[84] T. Morozumi, Y. Shimizu, S. Takahashi and H. Umeeda, PTEP **2018** (2018) no.4, 043B10.

[85] H. Y. Cheng, Phys. Rev. D **26**, 143 (1982).

[86] A. J. Buras, W. Slominski and H. Steger, Nucl. Phys. **B245**, 369 (1984).

[87] P. F. de Salas, D. V. Forero, S. Gariazzo, P. Martínez-Miravé, O. Mena, C. A. Ternes, M. Tórtola and J. W. F. Valle, JHEP **02**, 071 (2021).

[88] M. Tortola, Neutrinos global fit (2024), Talk at XV Latin American Symposium on High Energy Physics, URL <https://indico.nucleares.unam.mx/event/2125/contribution/40>.

[89] F. Capozzi, W. Giarè, E. Lisi, A. Marrone, A. Melchiorri and A. Palazzo, Phys. Rev. D **111** (2025) no.9, 093006.